Interdependence between Structural Engineering and Construction Management
Edited by Ozevin, D., Ataei, H., Modares, M., Gurgun, A., Yazdani, S., and Singh, A.

ISBN: 978-0-9960437-6-2

VISCOELASTIC ANALYSIS OF FLEXIBLE PAVEMENT EMBEDDED WITH CLSM BASES SUBJECTED TO SINUSOIDAL AND IMPULSIVE LOADS

YEN-CHU LIANG[1], HER-YUNG WANG[2], and LI-JENG HUANG[2]

[1]*Dept of Aeronautics and Astronautics, Air Force Academy, Kaohsiung, Taiwan (ROC)*
[2]*Dept of Civil Engineering, National Kaohsiung University of Science and Technology, Kaohsiung, Taiwan (ROC)*

This paper presents finite element analysis of 4-layered flexible pavements embedded visco-elastic asphalt concrete (AC) top layer and controlled low-strength materials (CLSM) sub-layers as well as graded crushed stone subgrades layers subjected to sinusoidal and impulsive surface wheel loads. Two-dimensional deformation assumption is employed. Time-dependent stress-strain relations are treated using Laplace transform based on correspondence principle. Scheme based on fast Fourier transform (FFT) is employed for inversion of Laplace transformed to obtain time-domain results. A typical 4-layered pavement is analyzed in which relaxation modulus of top visco-elastic asphalt layer is expressed in Prony series. Two kinds of CLSMs, i.e., CLSM-B80/30% and CLSM-B130/30% are compared with graded crushed stones and AC used for base materials. Time-domain responses of vertical displacement and stress at bottom of AC layer are compared. The vertical settlements using CLSM bases (B80/30% and B130/30%) are smaller than that using graded crushed stones even considering visco-elastic behavior of asphalt layer and show to be good materials employed as base substitutes for graded crushed stone in flexible pavement design.

Keywords: FEM, Numerical Laplace inversion, FFT, Asphalt concrete.

1 INTRODUCTION

Flexible pavements have been widely employed in highway engineering and effective rapid pavement construction had been achieved by using the controlled low strength materials (CLSM) (Lin *et al.* 2007, Bassani *et al.* 2015). CLSM is a kind of flowable fill defined as self-compacting cementitious material that is in a flowable state at the initial period of placement and has a specified compressive strength of 1200 psi or less at 28 days or is defined as excavatable if the compressive strength is 300 psi or less at 28 days as depicted in ACI-229R (2005). The CLSM is suitable for application to some pavements under repeated excavation and backfill is required such as pipeline construction. The authors had conducted some preliminary studies on engineering properties of CLSM (Huang *et al.* 2014) and the numerical analyses on static and free vibration analysis of CLSM bases in flexible pavements (Huang *et al.* 2017a, Huang *et al.* 2017b).

Asphalt mixtures have special viscoelastic behavior as depicted by Huang (1993). Their mechanical response exhibits time and rate dependency. Numerical schemes combined with finite element models and Laplace transform method or time-incremental skills have been applied

for flexible pavement analysis (Zocher *et al.* 1997, Evangelista *et al.* 2005, Malakouti *et al.* 2014). This study is aimed at visco-elastic analysis of 4-layered flexible pavements using finite element method. The top layer is considered as Hot Mix Asphalt (HMA), which is modeled as viscoelastic material; while 4 kinds of base materials are employed, i.e., graded crushed stones, CLSM-B80/30%, CLSM-B130/30% and AC. The numbers B80 and B130 mean the different levels of binder content (i.e. 80 and 130 kg/m^3) and different percentages fly ash (i.e. 30%) substituting to Portland cement were previously chosen for mix design. A comparison study is performed on time responses of vertical displacement and stress located at top of base layer under the sinusoidal and impulsive loadings.

2 FINITE ELEMENT MODELLING OF 4-LAYERED FLEXIBLE PAVEMENTS

Stress-strain relation of a visco-elastic material can be expressed in convolution integrals

$$\sigma(t) = E(t) \otimes \dot{\varepsilon}(t) = \int_0^t E(t-\tau) \bullet \frac{\partial \varepsilon}{\partial \tau} d\tau \tag{1a}$$

$$\varepsilon(t) = D(t) \otimes \dot{\sigma}(t) = \int_0^t D(t-\tau) \bullet \frac{\partial \sigma}{\partial \tau} d\tau \tag{1b}$$

For uni-axial stress state, where *E(t)* is the relaxation modulus, *D(t)* is the creep compliance, *t* is the current time, τ is a temporal variable. Taking Laplace transform of Eq. (1a) we have

$$\hat{\sigma}(s) = s\hat{E}(s) \bullet \hat{\varepsilon}(s) \tag{2}$$

From the correspondence principle in the theory of linear visco-elasticity, we can replace *E* by $s\hat{E}(s)$ in FEM and the calculations of nodal displacements and element stresses in Laplace transform domain are the same as for elastic analysis.

The relaxation modulus for a visco-elastic material can be expressed as the Prony series:

$$E(t) = E_\infty + \sum_{k=1}^{N} E_k \, e^{-t/\rho_k} \tag{3}$$

where E_∞, E_k, ρ_k are evaluated from experiment.

3 FFT FOR NUMERICAL LAPLACE INVERSION

There are various schemes developed for numerical Laplace inversion (Davies and Martin 1979). In this paper we employ the scheme based on FFT using integration of $\hat{F}(s)$ on imaginary axis with trapezoidal rule and expressed by Huddleston and Byrne (1999):

$$f(t_k) = \frac{1}{2\pi i} \int_{c-i\infty}^{c+i\infty} \hat{F}(s) \bullet e^{st_k} ds \approx \frac{e^{Ct_k}}{\pi} \sum_{j=1}^{N_\omega} \frac{1}{2} [\hat{F}(C + i\omega_j) \, e^{i\omega_j t_k} + \hat{F}(C + i\omega_{j+1}) \, e^{i\omega_{j+1} t_k}] \Delta\omega_j \tag{4}$$

where $s_j = C + i\omega_j$, C and ω_j denotes the real and imaginary parts of the complex-valued sampling points s_j. From the theory of Laplace inversion *C* should be located on the right-hand side of all poles of $\hat{F}(s)$.

4 NUMERICAL EXAMPLES

4.1 Validation of Viscoelastic Analysis Using FEM for a Visco-elastic Hollow Cylinder

We consider the thick-walled cylinder, with internal radius $a = 2m$ and external radius $b = 4m$, analyzed by previous researchers (Zocher *et al.* 1997, Evangelista *et al.* 2005), as shown in Figure 1. They analyzed the visco-elastic response for $p(t) = p_0 H(t)$ with $p_0 = 100\ Pa$. Visco-elastic material properties are: $E_\infty = 0.1 kPa,\quad E_1 = 0.4 kPa,\quad \rho_1 = 1.0 \sec,\quad \nu = 0.3$.

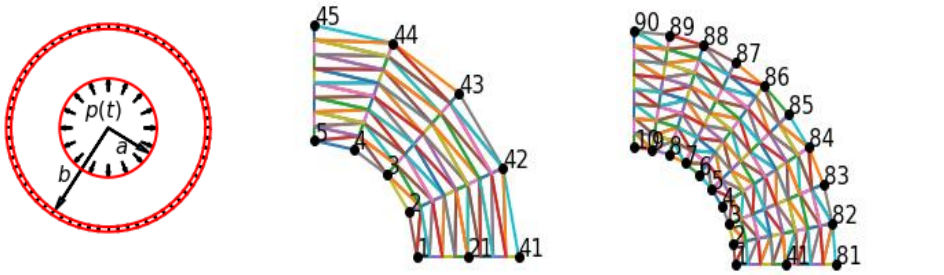

(a) Geometric model. (b) 64 triangular elements. (c) 144 triangular elements.

Figure 1. Geometric model and FEM meshes of the thick-walled visco-elastic cylinder.

4.1.1 *Sinusoidal pressure input*

For sinusoidal loading: $p(t) = p_0 \sin \Omega t$, where $\Omega = 0.5 rad/\sec$. The analytical solution is

$$u_r(t) = p_0 \frac{a^2 b(1+\nu)(1-2\nu)}{a^2 + (1-2\nu)b^2}\left(\frac{b}{r} - \frac{r}{b}\right) D_S(\Omega, t) \tag{5}$$

where,

$$D_S(\Omega, t) = \Omega\left[\frac{D_0 + D_1}{\Omega}\sin \Omega t + \frac{D_1}{\Omega^2 + 1/\lambda^2}\left(\frac{1}{\lambda} e^{-t/\lambda} - \frac{1}{\lambda}\cos \Omega t - \Omega \sin \Omega t\right)\right] \tag{6}$$

with $D_0 = 1/E_0,\ D_1 = (1/E_\infty - 1/E_0),\ \lambda_1 = E_0 \rho_1 / E_\infty,\ E_0 = E_\infty + E_1$.

The FEM predictions compared well with the analytical solutions as shown in Figure 2(a).

4.1.2 *Impulsive pressure input*

For impulsive pressure case: $p(t) = p_0\, \delta(t)$ is taken into account. The analytical solution is

$$u_r(t) = p_0 \frac{a^2 b(1+\nu)(1-2\nu)}{a^2 + (1-2\nu)b^2}\left(\frac{b}{r} - \frac{r}{b}\right)\frac{D_1}{\lambda} e^{-t/\lambda} \tag{7}$$

The comparison between the finite element solutions and the analytical solutions is good as shown in Figure 2(b). Polynomial fitting techniques with 3rd order are employed for impulsive oscillatory responses.

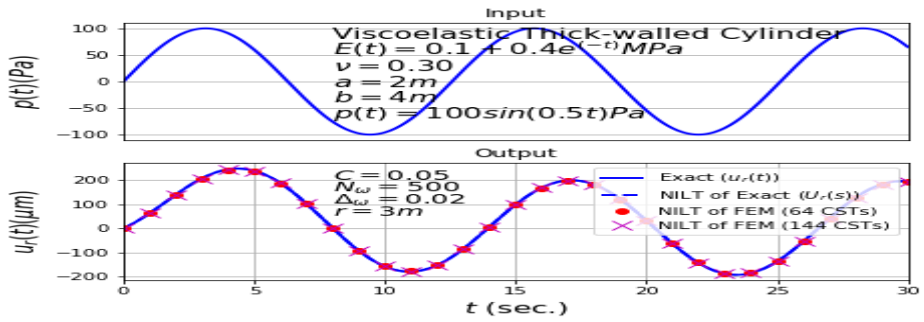

(a) Sinusoidal pressure input.

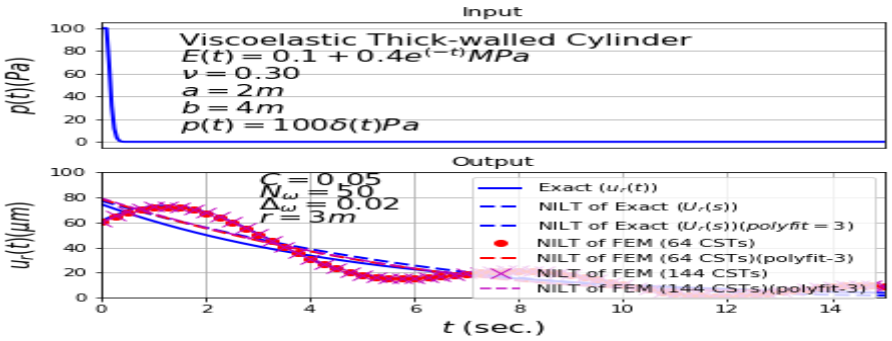

(b) Impulsive pressure input.

Figure 2. Comparison between FEM and analytical solutions for the thick-walled visco-elastic cylinder.

4.2 Visco-elastic Analysis of 4-layered Pavements

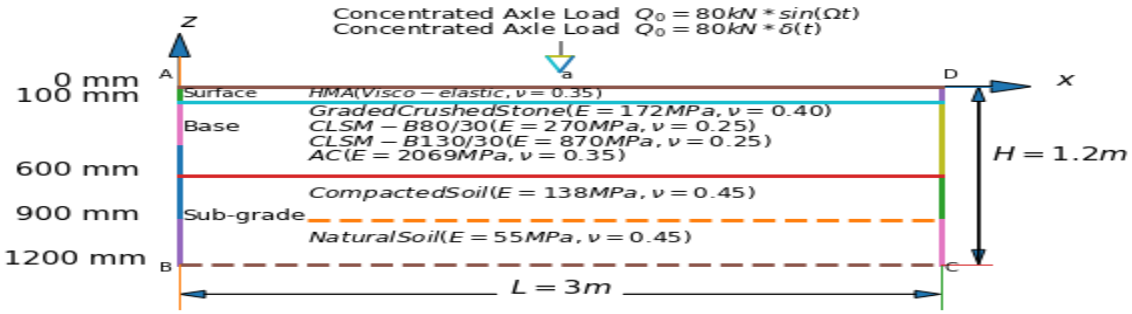

(a) Geometric model.

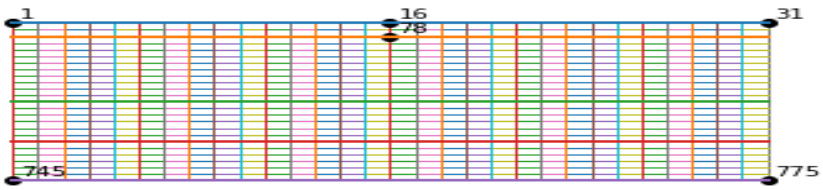

(b) 720 rectangular elements.

Figure 3. Geometric model and FEM meshes of the 4-layered pavements.

A 4-layered flexible pavement with different materials in base layer is illustrated in Figure 3(a). The material constants for AC, graded crushed stone, compacted soil and natural soil are the same as Chang and Chang (1998). The material constants for CLSM-B80/30% and CLSM-B130/30% are obtained from Sheen *et al.* (2014). Visco-elastic material properties in Prony series of the HMA layer are obtained from Lee (1996). Hinge supports along *AB*, *BC*, and *CD* are prescribed. Totally, *30×24=720 Q4* elements with *31×25=775* nodes are employed (Figure 3(b)).

4.2.1 *Sinusoidal vehicle loading*

The time-domain vertical displacements and stresses located at $(x, z) = (1.5m, -0.1m)$ (i.e., the node 78) due to sinusoidal vertical load are shown in Figure 4(a) and 4(b), respectively. The vertical settlements using CLSM bases (B80/30% and B130/30%) are smaller than that using graded crushed stones even considering visco-elastic behavior of top asphalt layer.

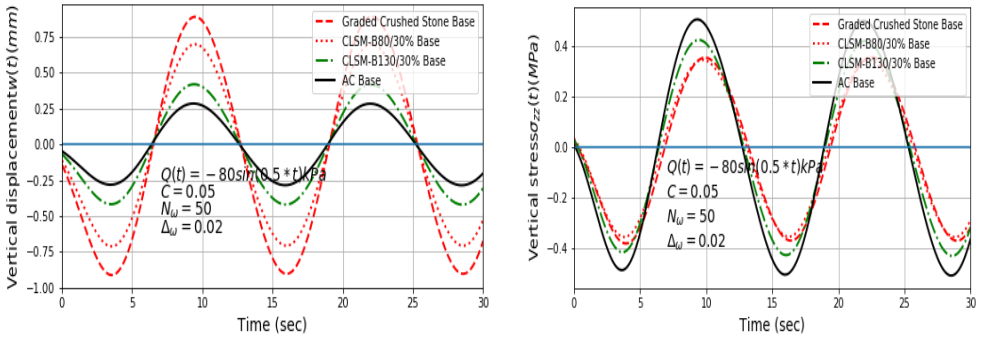

(a) Vertical displacement. (b) Vertical stress.

Figure 4. Displacements and stress of 4-layered flexible pavement for sinusoidal vehicle loading case.

4.2.2 *Impulsive vehicle loading*

The time-domain vertical displacements and stresses of the node 78 due to impulsive vertical load are shown in Figure 5(a) and 5(b), respectively. The vertical settlements using CLSM bases (B80/30% and B130/30%) are also smaller than that using graded crushed stones.

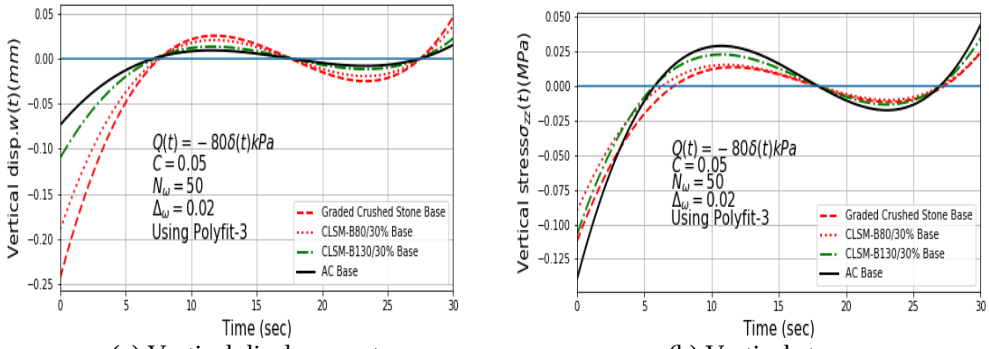

(a) Vertical displacement. (b) Vertical stress.

Figure 5. Displacements and stress of 4-layered flexible pavement for impulsive vehicle loading case.

5 CONCLUDING REMARKS

In this paper the finite element analyses of 4-layered flexible pavements with visco-elastic surface layer embedded with four different base materials subjected to surface sinusoidal and impulsive loads were studied. Correspondence principle and numerical Laplace inversion based on FFT is employed. The vertical displacement responses at top base layer using CLSMs are bounded by those using graded crushed stone base and AC base. The vertical settlements using CLSM bases (B80/30% and B130/30%) are smaller than that using graded crushed stones even considering visco-elastic behavior of asphalt layer.

References

ACI-229R, *Controlled Low-Strength Materials (Reproved 2005)*, Farmington Hills (MI) 2005.

Bassani, M., Khosravifar, S., Goulias, D. G., and Schwartz,C. W., Long-term Resilient and Permanent Deformation Behavior of Controlled Low-Strength Materials for Pavement Applications, *Journal of Transportation Geotechnics*, 2, 108-118, 2015.

Chang, D. W., and Chang, C. E., Study on Data Interpretation and Structural Index of Flexible Pavement, *Tamkang Journal of Science and Engineering*, 1(2), 83-96,1998.

Davies, B., and Martin, B., Numerical Inversion of the Laplace Transform: A Survey and Comparison of Methods, *Journal of Computational Physics*, 33, 1-32, 1979.

Evangelista, F., Parente, E., and Soares, J. B., *Visco-elastic and Elastic Structural Analysis of Flexible Pavements*, CILAMCE 2005-ABMEC & AMC, Guarapari, Espirito Santo, Brazil, October 19-21, 2005.

Huang, Y. H., *Pavement Analysis and Design*, Prentice-Hall, Inc., 1993.

Huang, L. J., Sheen, Y. N., and Le, D. H., *On the Multiple Linear Regression and Artificial Neural Networks for Strength Prediction of Soil-Based Controlled Low-Strength Material*, 3rd International Conference for Advanced Materials Design and Mechanics and Workshop on Android Robotics, Singapore, May 23-24, 2014.

Huang, L. J., Wang, H. Y., Huang, W. L., and Lin, M. C., *Finite Element Analysis of Controlled Low-Strength Material Pavement Bases Part I- Static Analysis*, ISEC-9, Resilient Structures and Sustainable Construction, Valencia, Spain, July 24-29, 2017a.

Huang, L. J., Wang, H. Y., Huang, W. L., and Lin, M. C., *Finite Element Analysis of Controlled Low-Strength Material Pavement Bases Part II- Free Vibration Analysis*, ISEC-9, Resilient Structures and Sustainable Construction, Valencia, Spain, July 24-29, 2017b.

Huddleston, T., and Byrne, P., Numerical Inversion of Laplace Transforms, University of South Alabama, April 1999. Retrieved from http://code.activestate.com/recipes/128243-numerical-inversion-of-laplace-transforms-using-the-fft-algorithm/ on January 2019.

Lee, H. J., *Uniaxial Constitutive Modeling of Asphalt Concrete Using Viscoelasticity and Continuum Damage Modeling*, PhD Dissertation, Department of Civil Engineering, North Caroline State University, Raleigh, NC, USA, 1996.

Lin, D. F., Luo, H. L., Wang, H. Y., and Hung, M. J., Successful Application of CLSM on a Weak Pavement Base/Subgrade for Heavy Truck Traffic, *Journal of Performance of Constructed Facilities*, 21(1), 70-77, 2007.

Malakouti, M., Ameri, M., and Malekzadeh, P., Incremental Layerwise Finite Element Formulation for Viscoelastic Response of Multilayered Pavements, *International Journal for Transportation Engineering*, 1(3), 183-198, 2014.

Sheen, Y. N., Huang, L. J. and Le, D. H., *Engineering Properties of Controlled Low-Strength Material Made with Residual Soil and Class F Fly Ash*, 3rd International Conference for Advanced Materials Design and Mechanics and Workshop on Android Robotics. Singapore, May 23-24, 2014.

Zocher, M. A., Groves, S. E., and Allen, D. H., Three-Dimensional Finite Element Formulation for Thermoviscoelastic Orthotropic Media, *International Journal for Numerical Methods in Engineering*, 40, 2267-2288, 1997.